

## Spark plasma sintering of Ni<sub>3</sub>Al-xB-1wt% CNT (0.0<x<1.5at%) nanocomposite

Mohammadnejad, A.; Bahrami, A.; Sajadi, M.; Mehr, M. Yazdan

**DOI**

[10.1016/j.jallcom.2019.02.225](https://doi.org/10.1016/j.jallcom.2019.02.225)

**Publication date**

2019

**Document Version**

Final published version

**Published in**

Journal of Alloys and Compounds

**Citation (APA)**

Mohammadnejad, A., Bahrami, A., Sajadi, M., & Mehr, M. Y. (2019). Spark plasma sintering of Ni<sub>3</sub>Al-xB-1wt% CNT (0.0<x<1.5at%) nanocomposite. *Journal of Alloys and Compounds*, 788, 461-467. <sup>3</sup>  
<https://doi.org/10.1016/j.jallcom.2019.02.225>

**Important note**

To cite this publication, please use the final published version (if applicable).  
Please check the document version above.

**Copyright**

Other than for strictly personal use, it is not permitted to download, forward or distribute the text or part of it, without the consent of the author(s) and/or copyright holder(s), unless the work is under an open content license such as Creative Commons.

**Takedown policy**

Please contact us and provide details if you believe this document breaches copyrights.  
We will remove access to the work immediately and investigate your claim.



# Spark plasma sintering of Ni<sub>3</sub>Al-xB-1wt% CNT (0.0 < x < 1.5 at%) nanocomposite



A. Mohammadnejad<sup>a</sup>, A. Bahrami<sup>a</sup>, M. Sajadi<sup>a</sup>, M. Yazdan Mehr<sup>b,\*</sup>

<sup>a</sup> Department of Materials Engineering, Isfahan University of Technology, Isfahan 84156-83111, Iran

<sup>b</sup> Faculty EEMCS, Delft University of Technology, Mekelweg 4, 2628 CD, Delft, the Netherlands

## ARTICLE INFO

### Article history:

Received 26 January 2019

Received in revised form

17 February 2019

Accepted 19 February 2019

Available online 22 February 2019

### Keywords:

Ni<sub>3</sub>Al

Carbon nanotubes

Mechanical properties

Spark plasma sintering

Nanocomposite

## ABSTRACT

This paper investigates the effects of carbon nanotubes (CNT) addition on the structure and mechanical properties of Ni<sub>3</sub>Al-xB (0.0 < x < 1.5 at%) intermetallic compound. Ni<sub>3</sub>Al-xB-1wt% CNT nanocomposite powders were first synthesized by mechanical alloying. Effects of CNT addition on the lattice strain and crystallite size of synthesized powders were investigated by means of X-ray diffraction (XRD) analysis. Scanning electron microscope (SEM) was used to study powder morphologies. Powders, synthesized by mechanical alloying, were then consolidated using spark plasma sintering (SPS), conducted at 950 °C under pressure 50 MPa. Microhardness and shear punch tests were employed to study the mechanical properties of sintered samples. Results show that CNT addition is accompanied by a decrease in crystallite size and a significant improvement of mechanical properties of Ni<sub>3</sub>Al-xB (0.0 < x < 1.5 at%) intermetallic compounds.

© 2019 Elsevier B.V. All rights reserved.

## 1. Introduction

Intermetallic compounds, including Ni<sub>3</sub>Al, are promising alloys for many high-temperature applications, including gas turbine blades and components of airplane engines [1–4]. Intermetallic alloys have several unique characteristics, such as superior high-temperature oxidation/corrosion resistance together with excellent microstructure stability during high temperature working conditions. In many cases, mechanical properties of intermetallic alloys are improved at temperature range 600–800 °C, making them an excellent choice when creep is the major concern [5]. There have been many attempts to improve the mechanical properties of Ni<sub>3</sub>Al compound by changing the chemistry of the alloy [6–8]. This includes the addition of boron, which reportedly significantly improves the mechanical properties of Ni<sub>3</sub>Al alloy [9]. What is certainly known about the implication of boron for the structure of Ni<sub>3</sub>Al is its contribution to the grain refinement, associated with an increase in the strength of the alloy. Yet, there is a controversy on the influence of boron on the ductility [10–12]. Further improvement in mechanical properties beyond what is achieved so far is still needed, given that advanced industries like

aerospace industries are getting more demanding than any time before. A well-known effective strengthening strategy when it comes to intermetallic alloys is grain refinement down to nanoscale range. Amongst different ways of doing so, mechanical alloying (MA) is certainly a promising one, given that it is a rather straightforward room temperature method with a great extent of controllability over crystallite/particle size [13–18]. This method is inherently less prone to manufacturing defects that one might have to deal with in other conventional manufacturing methods like casting or forging. Other prominent upsides of mechanical alloying are in-situ alloying during milling and a perfect homogeneity of alloying elements due to the repeated collision of particles in the course of milling. Meeting ever-increasing demands for advanced Ni<sub>3</sub>Al-based alloys of higher mechanical properties necessitates using a dispersion of nanoparticles to get a contribution from dispersion hardening. Mechanical alloying is potentially an ideal way of achieving a rather homogeneous distribution of nano-sized dispersoids in the matrix. Amongst different possible second phase particles, carbon nanotubes (CNTs) have shown great potential in improving mechanical properties and stiffness of a wide range of metal-matrix composites [19–22]. CNT has been successfully applied to not only different metals but also some intermetallic alloys [14].

Solid-state consolidation techniques are widely used methodologies to achieve fully dense materials from initial powders. These

\* Corresponding author.

E-mail address: [m.yazdanmehr@tudelft.nl](mailto:m.yazdanmehr@tudelft.nl) (M.Y. Mehr).

methods are less prone to the type of defects; one can normally anticipate in liquid-state processing. Yet, the downside of many of conventional solid-state hot pressing methodologies is their relatively long processing time which implicates that the powders stay at high temperature for a long time. This, in case of improper control, results in grain growth which in turn deteriorates mechanical properties of the final product. An alternative approach with minimized grain growth is spark plasma sintering (SPS). This approach, which is essentially a pressure-driven densification method under pulsed electric current in graphite dies, is considered as one of the fastest densification methods, if not the fastest one [20]. Fig. 1 shows schematics of an SPS machine. In this study, microstructure and mechanical properties of  $\text{Ni}_3\text{Al}$  alloy with various

amounts of boron addition (0.0, 0.5, 1.0 and 1.5 at%) and 1 wt% of multi-wall carbon nanotubes (MWCNTs), synthesized by mechanical alloying and spark plasma sintering, are investigated. The correlation between structure, milling/sintering parameters, and the mechanical properties of alloys will be discussed.

## 2. Materials and methods

Nickel (99.9% purity, 3  $\mu\text{m}$  average size), Aluminum (99.9% purity, 22  $\mu\text{m}$  average size), Boron (99.5% purity, 2  $\mu\text{m}$  average size) and Carbon Nano Tube (Multi-wall, 99.0% purity, 10 nm outer diameter) particles were used as initial elemental powders to synthesize  $\text{Ni}_3\text{Al-xB-1wt.\% MWCNT}$  ( $0.0 < x < 1.5$  at%). SEM images of initial particles together with the XRD spectrum of the initial powder mixture are shown in Fig. 2. Milling was done in two stages; at first, metallic powders were mixed and milled up to 35 h, to synthesize boron-containing  $\text{Ni}_3\text{Al}$  compounds. Then, in order to achieve a homogeneous distribution of elements and to minimize agglomeration of CNTs, synthesized powders together with CNTs were sonicated in ethanol (99.0% purity) for 30 min. Then, the mixture was dried in an oven at 80  $^\circ\text{C}$  for an hour. The dried mixture was then milled for another 5 h. Mechanical alloying was conducted in a steel vial with a rotation speed of 350 rpm in Argon atmosphere to prevent oxidation. A combination of balls was used for milling; 4 balls of 20 mm diameter, 3 balls of 12 mm diameter, and 2 balls of 10 mm diameter. In all experiments, the ball to powder ratio was chosen to be 10:1. Milling was interrupted every 10 h to take samples out for structural characterization. X-ray diffractometry (XRD, Philips,  $\text{Cu K}\alpha = 1.54$  nm) analysis was done on powders to characterize phase formation and to calculate lattice strain and crystallite size (XRD spectrum of the initial powder mixture is shown in Fig. 2d). Details on how these parameters are calculated are explained in here [10]. Scanning electron microscopy (SEM, Philips) analysis was also done to observe the morphology and particle size of powders with and without CNT. Mechanically

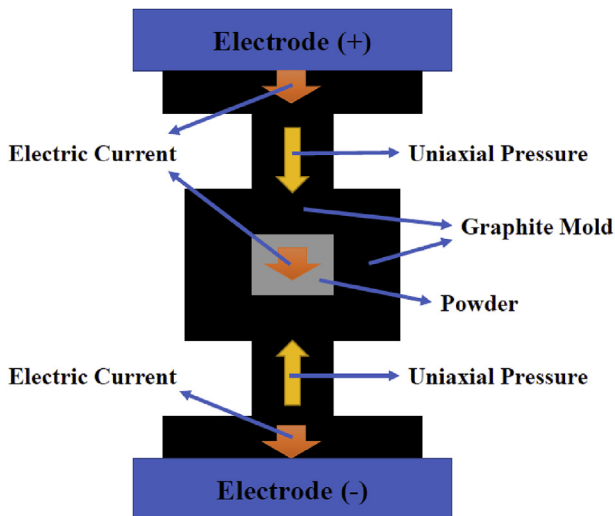


Fig. 1. Schematics of an SPS machine.

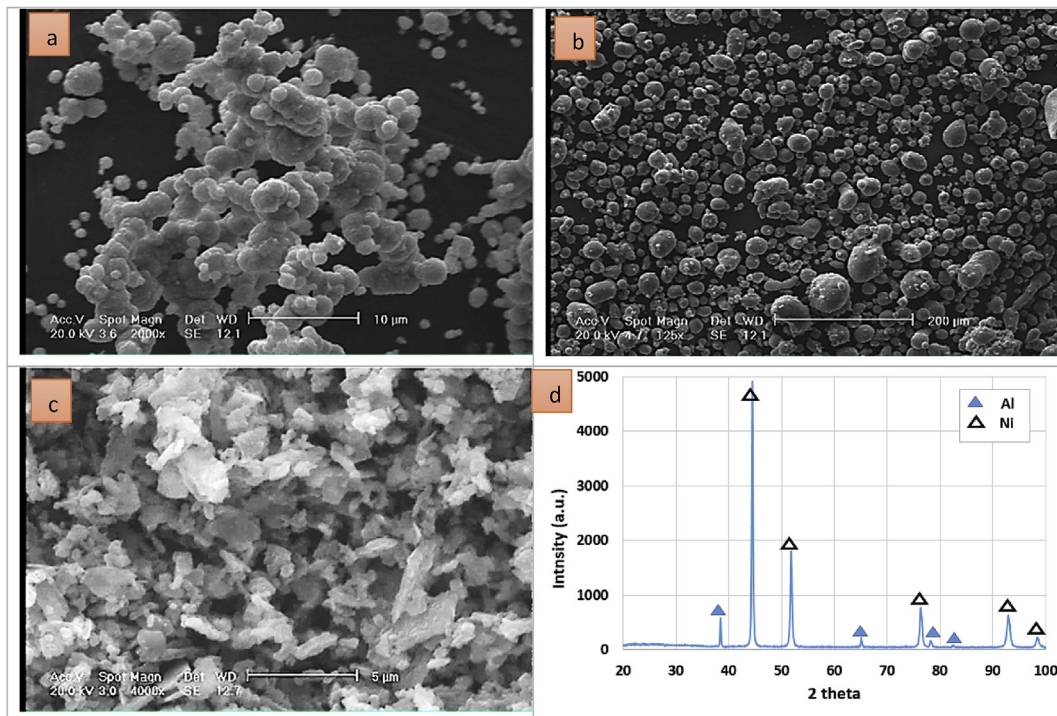


Fig. 2. SEM images of a) Ni, b) Al and c) B as initial powders, and d) XRD spectrum of Ni and Al initial mixtures.

alloyed powders were then consolidated using Spark Plasma Sintering (SPS, KPF vacuum technology) method, with uniaxial pressure of 50 MPa, at temperature 950 °C, with 10 min as holding time. Both heating and cooling rates were 100 °C/min. To examine mechanical properties, Vickers micro-hardness (0.1 Kg force), and shear-punch tests were used. Punch diameter in the shear-punch test was 3 mm with a rate of 0.1 m/s. The fracture surface of specimens after shear was studied by SEM and field emission scanning electron microscopy (FESEM).

### 3. Results

#### 3.1. Synthesis of $Ni_3Al-xB-1wt\%CNT$ ( $0.0 < x < 1.5$ at%) compounds

Fig. 3 shows XRD patterns of  $Ni_3Al-xB$  ( $x = 0.5$  and 1.5 at%) compounds with and without CNT after 40 h of mechanical alloying. The diffraction spectra of powders show peaks corresponding to  $Ni_3Al$  compound, indicating that 40 h of milling is enough to transform elemental powders to  $Ni_3Al$  compound. Elemental mapping of alloy  $Ni_3Al-1.5$  at%B after 40 h of milling confirms a perfectly homogeneous distribution of alloying elements (see Fig. 4). From XRD spectra, it appears that the addition of nano-sized CNT into  $Ni_3Al-xB$  ( $x = 0.5, 1.0,$  and 1.5 at%) alloys resulted in further broadening of  $Ni_3Al$  peaks. Mechanical alloying

is known to cause a significant peak broadening [10]. It appears that this effect is more pronounced in the presence of CNT. The increase in full width at half maximum (FWHM) of XRD peaks, induced by CNT addition, is not a fixed value at different boron contents. The CNT-induced increase in peak width of  $Ni_3Al-0.5$  at%B,  $Ni_3Al-1.0$  at%B, and  $Ni_3Al-1.5$  at%B samples are approximately 20, 30, and 60% respectively, inferring that the higher the boron content, the more pronounced the effect of CNT addition is. In addition to peak broadening, a minor shift in the position of XRD peaks towards lower angles is also noticed, which has to do with the lattice distortion during milling. Table 1 gives the values of crystallite size and lattice strains. The way how these values are calculated from XRD spectra is explained in here [10]. One can see that CNT addition is associated with a significant decrease in grain size and a significant increase in lattice strain in all boron contents. CNT addition can interestingly decrease crystallite size to values as low as 10 nm.

SEM images of particles, milled for 40 h, are shown in Fig. 5. This figure shows the effect of CNT addition on the particle size and morphology of powders. Obviously, the spherical shape of particles does not change by the addition of CNT. However, the particle size is greatly influenced by CNTs. CNT addition results in more refined particles with narrower size distribution. This effect is more pronounced in  $Ni_3Al-0.5B$  and  $Ni_3Al-1.0B$  compounds. In the former the average particle size decreases from 9 to 6  $\mu m$ , whereas in the latter it changes from 7 to almost 5  $\mu m$ . In case of alloy  $Ni_3Al-1.5B$ , the effect is marginal and insignificant. It appears that CNT addition not only decreases grain size but also slightly decreases particle size.

#### 3.2. Spark plasma sintering of synthesized powders

Fig. 6 shows the effects of CNT addition on the porosity percentages in sintered specimens (The area fraction of porosities was measured by the image analyzing of optical metallography images). Fig. 6b and c shows optical microscope images of  $Ni_3Al-0.5B$  and  $Ni_3Al-0.5B-CNT$  samples in as-polished condition respectively. The former alloy, containing CNT, clearly has less porosity. It appears that both boron and CNT additions decrease the porosity percentage of consolidated samples [10]. The effect of the latter is more pronounced. Up to 30% more reduction in porosity content can be achieved when CNT is added to the matrix. Effects of CNT and boron additions on the porosity percentages are more pronounced when the boron content is increased to 0.5 at%. Both boron and CNT introduce lattice distortions and this enhances the kinetics of diffusion of alloying elements during sintering. The faster the kinetics of diffusion, the faster is the kinetics of sintering, knowing that sintering is a diffusion-controlled reaction.

Fig. 7 shows the effects of CNT addition on the shear strength and hardness of  $Ni_3Al-xB$  compounds. As shown, samples with higher boron contents show less ductility and break at lower elongations. CNT increases the elongation of all specimens. Over 20% increase in elongation is achieved in CNT-containing specimens. Interestingly, CNT increases the elongation, while it does not deteriorate maximum shear strength. In the case of  $Ni_3Al-1.0B$ , CNT addition is associated with a significant increase in maximum shear strength. This also applies to hardness, where CNT addition significantly improves the hardness of bulk samples. Fig. 8 shows the influence of CNT addition on the fracture surface of  $Ni_3Al-1.0B$  sample. CNT addition clearly changes the fracture from a cleavage fracture to a more ductile fracture with a distribution of very fine dimples. A closer look at the fracture surface reveals some areas in which still there are some colonies of CNTs left in the microstructure (see Fig. 9).

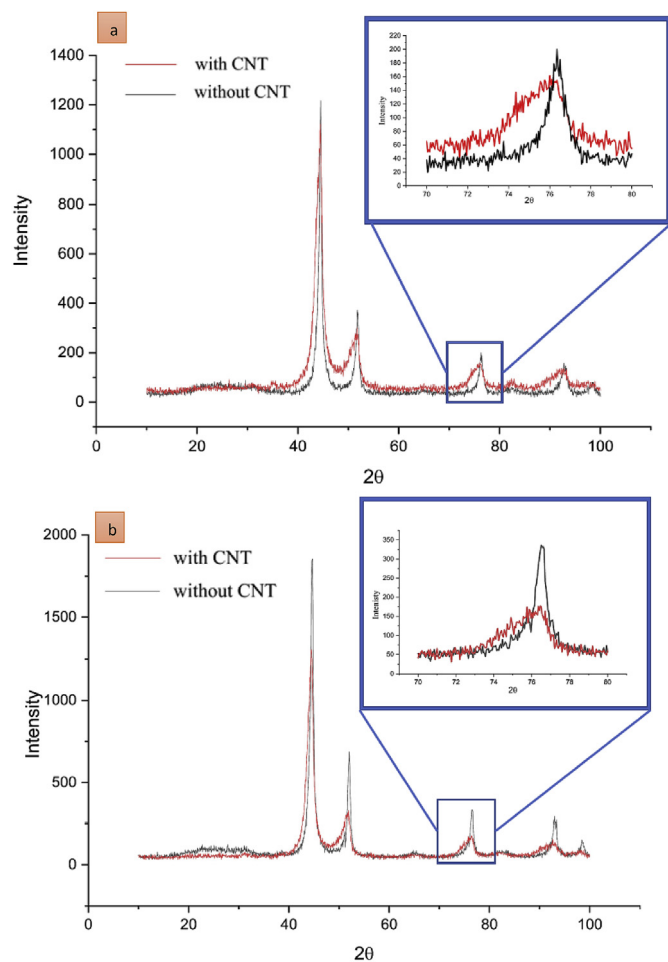


Fig. 3. Comparison between XRD analysis patterns of a)  $Ni_3Al-0.5$  at%B and b)  $Ni_3Al-1.5$  at%B compounds, with and without CNT addition (The XRD pattern of  $Ni_3Al-1.0$  at%B is similar to these two spectra).

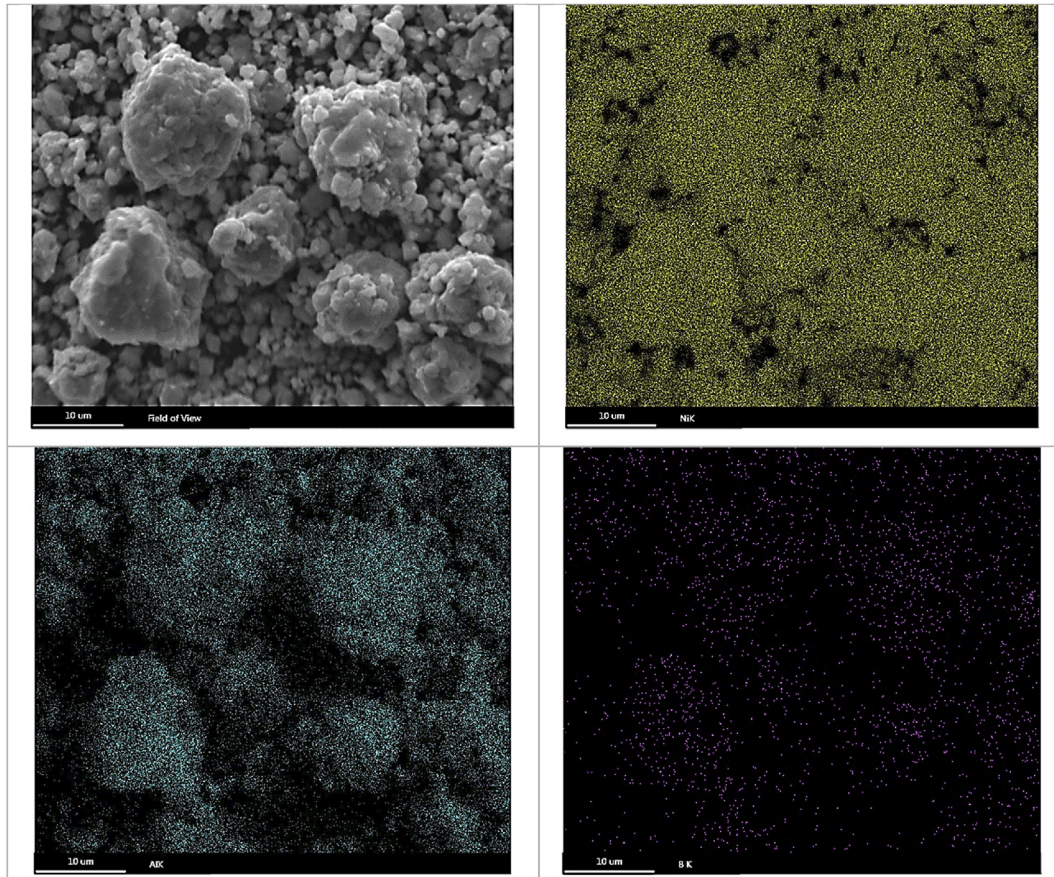


Fig. 4. Elemental mapping of Ni<sub>3</sub>Al-1.5 at%B compound after 40 h of milling.

#### 4. Discussion

This paper investigates the influence of CNT addition on the structure and mechanical properties of Ni<sub>3</sub>Al-*x*B alloys, synthesized by mechanical alloying and spark plasma sintering. CNT with exceptional physical and mechanical properties has shown great potential as a reinforcing component to improve the mechanical, electrical and thermal properties of composites [20]. Nickel aluminide compounds are now widely used for many high-temperature applications, due to their excellent mechanical properties and superior high-temperature oxidation/corrosion resistance [2]. Mechanical alloying is a solid-state alloying technique in which the ball/powder collisions during milling induces interdiffusion of alloying elements associated with distortion of crystal structure and grain refinement [5]. Mechanical milling of elemental Ni and Al powders at the early stage of milling results in the formation of a Ni (Al) solid solution [23]. Mechanical milling up to 30 h leads to the formation of Ni<sub>3</sub>Al compound [10]. Results of our previous study [10] show Further milling is associated with a significant decrease in the crystallite size of Ni<sub>3</sub>Al compound. The kinetics of grain refinement gets slower by increasing the milling time, and at some point around 13–15 nm (depending on the boron content of the alloy), further milling hardly decreases crystallite

size. On the contrary, it might even cause a slight grain growth [10], which has to do with temperature increase at the ball/powders interface. The upside of mechanical alloying is the perfectly homogeneous distribution of alloying elements in the synthesized compounds, which in turn results in a homogeneous microstructure and phase distribution. Fig. 4 shows how homogeneous alloying elements are distributed in the mechanically alloyed sample (after 40 h of milling). There is obviously absolutely no indication of segregation or colonies of alloying elements. Homogeneous dispersion of elements is extremely important when it comes to the successful addition of CNT to the Ni<sub>3</sub>Al-*x*B matrix. It is postulated [14] that homogeneous dispersion of CNTs in the matrix is an essential step to get the highest mechanical properties. Results of this study show that CNT-containing Ni<sub>3</sub>Al-*x*B samples have overall a significantly smaller grain size (down to 10 nm) compared to samples without CNT. Observed peak broadening in XRD spectra conclusively implicates that CNT (partly) enters into the crystal structure of the base alloy and this causes further grain refinement. The CNT-assisted decrease in grain size is in the order of 20–30%, depending on the boron content of the alloy. Observed grain refinement, combined with a solid solution and dispersion strengthening effects of CNT nanoparticles, results in a significant improvement of hardness (see Fig. 7d).

**Table 1**  
Crystallite size and lattice strains of mechanically alloyed powders.

| Samples         | Ni <sub>3</sub> Al-0.5B | Ni <sub>3</sub> Al-0.5B-CNT | Ni <sub>3</sub> Al-1.0B | Ni <sub>3</sub> Al-1.0B-CNT | Ni <sub>3</sub> Al-1.5B | Ni <sub>3</sub> Al-1.5BCNT |
|-----------------|-------------------------|-----------------------------|-------------------------|-----------------------------|-------------------------|----------------------------|
| Grain Size (nm) | 15.7                    | 10.2                        | 13.7                    | 10.3                        | 14.6                    | 9.8                        |
| Lattice Strain  | 0.52                    | 0.71                        | 0.70                    | 0.87                        | 0.65                    | 0.89                       |

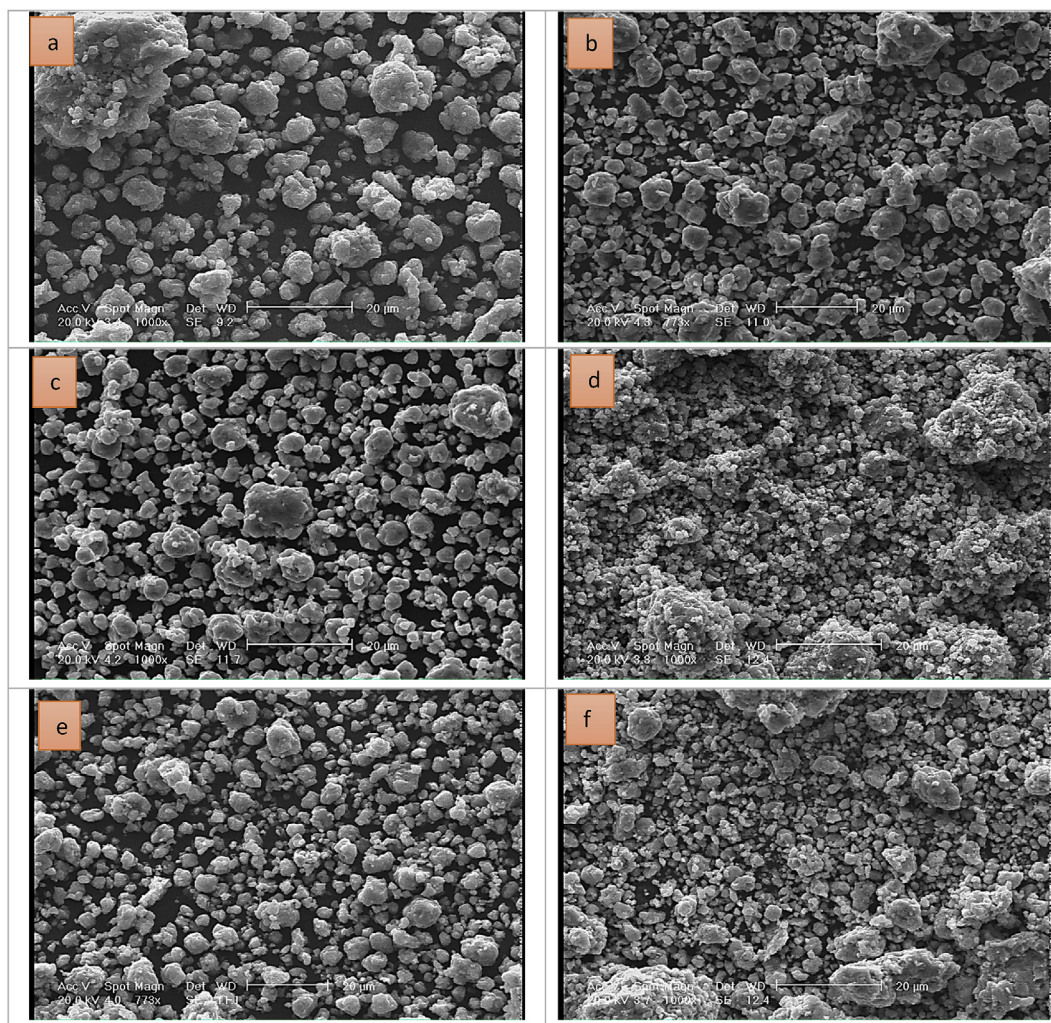


**Fig. 5.** SEM images of particles after 40 h of milling in a) Ni<sub>3</sub>Al-0.5B, b) Ni<sub>3</sub>Al-0.5B-1wt%CNT, c) Ni<sub>3</sub>Al-1.0B, d) Ni<sub>3</sub>Al-1.0B-1wt%CNT, e) Ni<sub>3</sub>Al-1.5B, and f) Ni<sub>3</sub>Al-1.5B-1wt%CNT compounds.

It appears that CNT addition not only decreases grain size but also has some implications for the particle size. CNT-containing samples have a comparatively smaller particle size, compared to samples without CNT. It is hypothesized that the high density of defects in mechanically alloyed powders increases energy transfer during ball-powder collisions [24]. Entering carbon into the matrix increases the level of lattice strain and this leads to a higher energy transfer from collisions to powders and smaller particle size. CNT addition also decreases the porosity percentages. The higher the lattice distortion, the easier is the diffusion of alloying elements. This enhanced diffusion of alloying elements increases the kinetics of sintering and this obviously decreases porosity percentages of the final bulk samples. Results of shear punch test on Ni<sub>3</sub>Al-xB alloys in our previous study [10] showed that boron additions higher than 0.5 at% results in a significant deterioration of ductility. On the contrary, CNT interestingly improves the ductility of Ni<sub>3</sub>Al-xB alloys. CNT particles, entered into the crystal structure, are expected to diffuse towards grain boundaries as well in which case they decrease the order of crystal structure of the intermetallic at the grain boundary. It is known that a decrease of ordered intermetallic phase at grain boundaries is associated with higher degree of dislocation mobility and this means higher ductility [25]. Given that grain boundary failure is believed to be the main reason for observed brittleness in Ni<sub>3</sub>Al alloys [26], one can conclude that

carbon diffusion-induced disordering of grain boundary structure has an essential contribution to the observed improvement of ductility. The effect of CNT addition on the ductility of Ni<sub>3</sub>Al-xB alloys is very well reflected on the fracture surface as well (see Fig. 8). While Ni<sub>3</sub>Al-xB alloys show a brittle cleavage fracture surface, samples containing CNT show a more ductile fracture, confirmed by the distribution of fine dimples at the fracture surface.

## 5. Conclusions

From the results obtained in this investigation, the following conclusions can be drawn:

- CNT addition is associated with a significant grain refinement of Ni<sub>3</sub>Al-xB (0.0 < x < 1.5 at%) alloys, down to 10 nm. This is confirmed by peak broadening in XRD spectra.
- The observed shift in the position of XRD peaks infers that part of CNT enters into the crystal structure of base alloy and displaces atoms from their equilibrium positions.
- CNT addition also slightly decreases the particle size, which has to do with the fact that CNT introduction to the matrix induces lattice distortion and this increases energy absorption in ball/powder collisions.

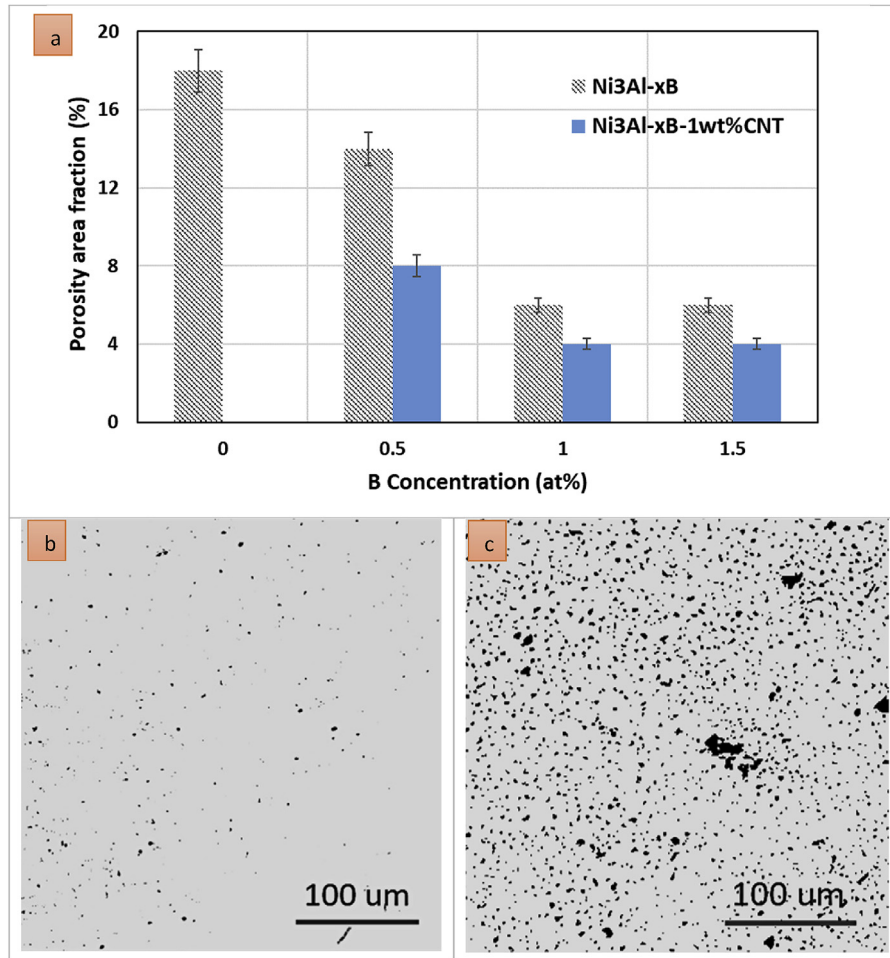


Fig. 6. a) Effects of CNT addition on the porosity percentage of sintered specimens (The area fraction of porosities are measured using an image analyzing technique), an example related to b) alloy Ni3Al-0.5B-CNT, and c) Ni3Al-0.5B.

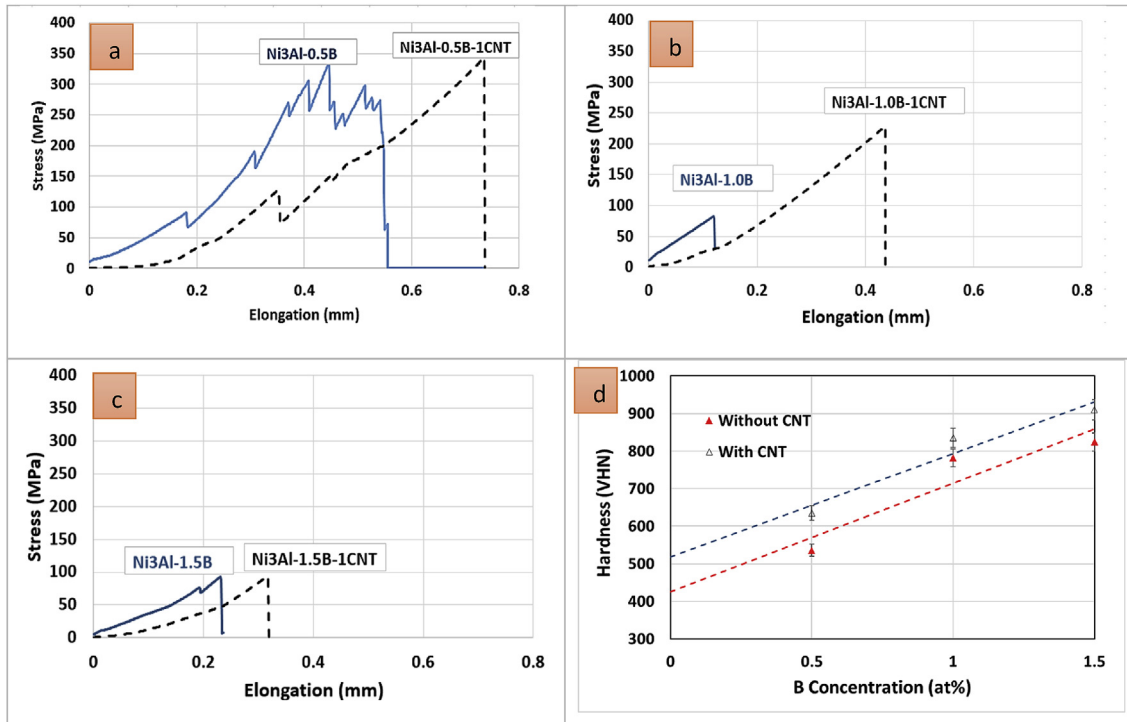


Fig. 7. Effects of CNT addition on the shear strength and hardness of Ni3Al-xB samples.

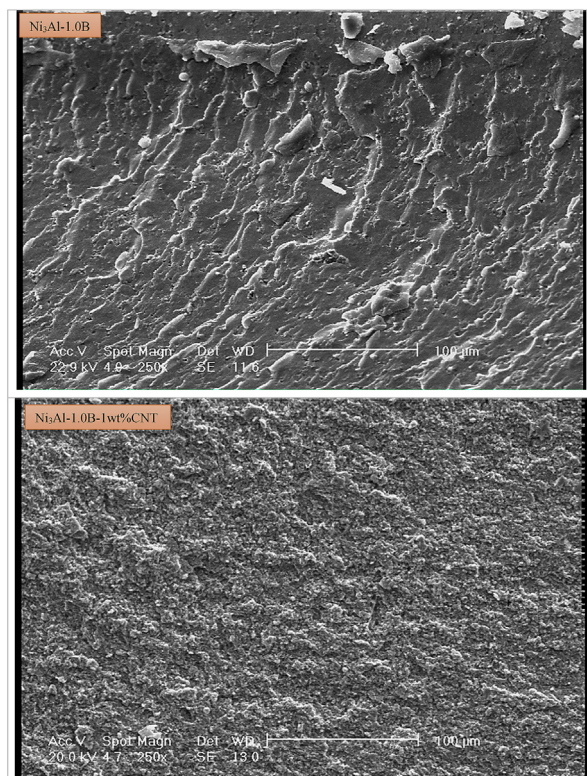


Fig. 8. Effects of CNT addition on the fracture surface of Ni<sub>3</sub>Al-1.0B sample.

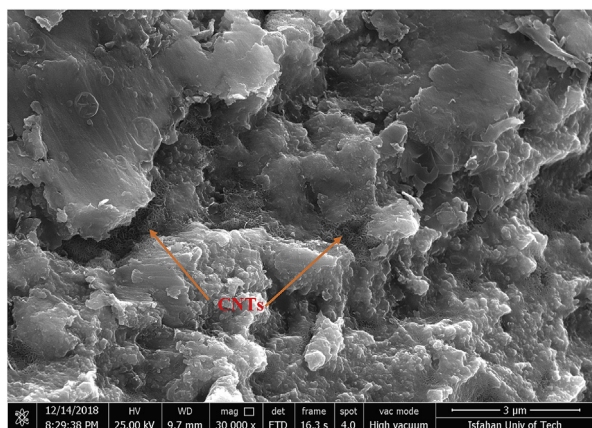


Fig. 9. Effects of CNT addition on the fracture surface of Ni<sub>3</sub>Al-1.0B sample.

- Samples containing CNTs shows a comparatively lower percentage of porosity. Lattice distortion, induced by introduction of CNTs into the base alloy, eases the diffusion of alloying elements, resulting in faster kinetics of sintering.
- CNT addition improves the hardness of sintered Ni<sub>3</sub>Al-xB (0.0 < x < 1.5 at%) alloys. This has to do with grain refinement, induced by CNT addition, combined with dispersion and solid solution strengthening effects of CNTs.
- CNT addition to Ni<sub>3</sub>Al-xB (0.0 < x < 1.5 at%) alloys is associated with a significant improvement of ductility. This is believed to be due to disordering of crystal structure at the grain boundary, caused by diffusion of carbon towards grain boundaries. \

## References

- [1] K. Bochenek, M. Basista, Advances in processing of NiAl intermetallic alloys and composites for high-temperature aerospace applications, *Prog. Aero. Sci.* 79 (2015) 136–146.
- [2] P. Jóźwik, W. Polkowski, Z. Bojar, Applications of Ni<sub>3</sub>Al based intermetallic alloys—current stage and potential perceptivities, *Materials* 8 (5) (2015) 2537–2568.
- [3] W. Polkowski, P. Jóźwik, Z. Bojar, EBSD and X-ray diffraction study on the recrystallization of cold rolled Ni<sub>3</sub>Al based intermetallic alloy, *J. Alloys Compd.* 614 (2014) 226–233.
- [4] V.K. Sikka, S.C. Deevi, S. Viswanathan, R.W. Swindeman, M.L. Santella, Advances in processing of Ni<sub>3</sub>Al-based intermetallics and applications, *Intermetallics* 8 (2000) 1329–1337.
- [5] C. Suryanarayana, Mechanical alloying and milling, *Prog. Mater. Sci.* 46 (1–2) (2001) 1–184.
- [6] S. Ito, T. Yoshikawa, S. Miyazawa, K. Mori, Machinability of Ni<sub>3</sub>Al-based intermetallic compounds, *J. Mater. Process. Technol.* 63 (1997) 181–186.
- [7] M. Li, J. Song, Y. Han, Effects of boron and carbon contents on long-term aging of Ni<sub>3</sub>Al-base single crystal alloy IC6SX, *Proced. Eng.* 27 (2012) 1054–1060.
- [8] M.L. Huang, C. Yu Wang, Effects of boron and carbon on the ideal strength of Ni solution and Ni<sub>3</sub>Al intermetallics: a first-principles study of tensile deformation, *Comput. Mater. Sci.* 140 (2017) 140–147.
- [9] N. Masahashi, Physical and mechanical properties in Ni<sub>3</sub>Al with and without boron, *Mater. Sci. Eng., A* A223 (1997) 42–53.
- [10] A. Mohammadnejad, A. Bahrami, M. Sajadi, P. Karimi, H.R. Fozveh, M. Yazdan Mehr, Microstructure and mechanical properties of spark plasma sintered nanocrystalline Ni<sub>3</sub>Al-xB (0.0 < x < 1.5 at%) alloy, *Mater Today Commun.* 17 (2018) 161–168.
- [11] J. Meng, C. Jia, Q. He, Effect of mechanical alloying on the structure and property of Ni<sub>3</sub>Al fabricated by hot pressing, *J. Alloys Compd.* 421 (2006) 200–203.
- [12] Y. Yua, J. Zhou, J. Chena, H. Zhou, C. Guoa, B. Guoc, Synthesis of nanocrystalline Ni<sub>3</sub>Al by mechanical alloying and its microstructural characterization, *J. Alloys Compd.* 498 (2010) 107–112.
- [13] C. Suryanarayana, Nasser Al-Aqeeli, Mechanically alloyed nanocomposites, *Prog. Mater. Sci.* 58 (2013) 383–502.
- [14] S. Ameri, Z. Sadeghian, I. Kazeminezhad, Effect of CNT addition approach on the microstructure and properties of NiAl-CNT nanocomposites produced by mechanical alloying and spark plasma sintering, *Intermetallics* 76 (2016) 41–48.
- [15] G. Cao, L. Geng, Z. Zheng, M. Naka, The oxidation of nanocrystalline Ni<sub>3</sub>Al fabricated by mechanical alloying and spark plasma sintering, *Intermetallics* 15 (2007) 1672–1677.
- [16] M.H. Enayati, Z. Sadeghian, M. Salehi, A. Saidi, The effect of milling parameters on the synthesis of Ni<sub>3</sub>Al intermetallic compound by mechanical alloying, *Mater. Sci. Eng., A* 375–377 (2004) 809–811.
- [17] A. Antolak-Dudka, M. Krasnowski, S. Gierlotka, T. Kulik, Nanocrystalline Ni<sub>3</sub>Al-based alloys obtained by recycling of aluminium scraps via mechanical alloying and consolidation, *Adv. Powder Technol.* 27 (2016) 305–311.
- [18] A. Bahrami, H.R. Madaah Hosseini, P. Abachi, S. Miraghaei, Structural and soft magnetic properties of nanocrystalline Fe<sub>85</sub>Si<sub>10</sub>Ni<sub>5</sub> powders prepared by mechanical alloying, *Mater. Lett.* 60 (2006) 1068–1070.
- [19] H. Deng, J. Yi, C. Xia, Y. Yi, Mechanical properties and microstructure characterization of well-dispersed carbon nanotubes reinforced copper matrix composites, *J. Alloys Compd.* 727 (2017) 260–268.
- [20] A. Azarniya, A. Azarniya, S. Sovizi, H.R. Madaah Hosseini, T. Varol, A. Kawasaki, S. Ramakrishna, Physicomechanical properties of spark plasma sintered carbon nanotube-reinforced metal matrix nanocomposites, *Prog. Mater. Sci.* 90 (2017) 276–324.
- [21] K.S. Munir, Y. Zheng, D. Zhang, J. Lin, Y. Li, C. Wen, Improving the strengthening efficiency of carbon nanotubes in titanium metal matrix composites, *J. Mater. Sci. Eng., A* 696 (2017) 10–25.
- [22] A.J. Albaaji, E.G. Castle, M.J. Reece, J.P. Hall, S.L. Evans, Effect of ball-milling time on mechanical and magnetic properties of carbon nanotube reinforced FeCo alloy composites, *Mater. Des.* 122 (15) (2017) 296–306.
- [23] M. Abbasi, S.A. Sajjadi, M. Azadbeh, An investigation on the variations occurring during Ni<sub>3</sub>Al powder formation by mechanical alloying technique, *J. Alloys Compd.* 497 (2010) 171–175.
- [24] S. Sivasankaran, K. Sivaprasad, R. Narayanasamy, P.V. Satyanarayana, X-ray peak broadening analysis of AA 6061<sub>100-x</sub>-x wt.%Al<sub>2</sub>O<sub>3</sub> nanocomposite prepared by mechanical alloying, *Mater. Char.* 62 (2011) 661–672.
- [25] A.H. King, M.H. Yoo, High temperature ordered intermetallic alloys H, in: N.S. Stoloff, C.C. Koch, C.T. Liu, O. Izumi (Eds.), *Materials Research Society Symposia Proceedings*, vol. 81, Materials Research Society, Pittsburgh, 1987, pp. 45–53.
- [26] F.E. Heredia, D.P. Pope, Effect of boron additions on the ductility and fracture behavior on Ni<sub>3</sub>Al single crystals, *Acta Metall. Mater.* 39 (8) (1991) 2017–2026.